

## Nomogram for Aiding the Interpretation of Tornadic Vortex Signatures Measured by Doppler Radar

RODGER A. BROWN

*NOAA, National Severe Storms Laboratory, Norman, Oklahoma*

28 February 1997 and 17 December 1997

### ABSTRACT

A technique is described whereby an investigator can obtain a more representative peak velocity for a tornadic vortex signature (TVS) than can be obtained by using the extreme measured Doppler velocities associated with the signature. This technique, which is based on theoretical curves derived by scanning a simulated radar through Rankine combined vortices, is applied to WSR-88D Doppler velocity data collected in the Garden City, Kansas, tornado of 16 May 1995. The technique produces peak TVS velocities that are more consistent in time and height than those computed directly from the extreme measured values.

### 1. Introduction

When a Doppler radar transmits a pulse, the angular width of the narrow beam remains constant, while the beam's physical width increases linearly with range from the radar. The width of the beam relative to the size of a sampled feature affects the sampling resolution. As the radar scans across the center of a vertical vortex whose horizontal dimension is significantly larger than the radar beamwidth, the Doppler velocity measurements are a good representation of velocity distribution across the vortex. However, with increasing width of the radar beam relative to a given-sized vortex, the peak Doppler velocity measurements progressively underestimate the peak tangential velocities of the vortex (e.g., Donaldson 1970; Brown and Lemon 1976). When the beamwidth is larger than the vortex's core diameter (where the peak tangential velocities are found), the characteristics of the vortex are so degraded that the peak Doppler velocity measurements no longer bear any resemblance to the peak tangential velocities or core diameter of the vortex (e.g., Brown et al. 1978). In fact, the peak Doppler velocity values are separated by about one beamwidth, regardless of the size or strength of the subbeam vortex.

Within a severe thunderstorm, two different types of vortices are commonly found—the mesocyclone and the tornado—which, in turn, produce four different kinds of Doppler velocity signatures, depending on the size of the radar beam relative to the core diameter of the vortex.

- 1) tornado signature—a rare vortex signature of extreme Doppler velocity values (of opposite sign) separated by at least several beamwidths in the azimuthal direction, which arises when the tornado is within a few kilometers of the radar and the tornado is larger than the radar beam;
- 2) tornadic vortex signature (TVS)—a vortex signature of degraded Doppler velocity extremes (of opposite sign) separated by about one beamwidth in the azimuthal direction, which arises when the radar beam is wider than the tornado; characteristics of the tornado are degraded to such an extent that neither the size nor strength of the tornado is recoverable (Brown et al. 1978);
- 3) mesocyclone signature—a vortex signature of extreme Doppler velocity values (of opposite sign) separated by approximately 3–10 km in the azimuthal direction, that arises when the mesocyclone is larger than the radar beam;
- 4) mesocyclonic vortex signature—analogue to the TVS, a vortex signature of degraded Doppler velocity extremes (of opposite sign) separated by about one beamwidth in the azimuthal direction, which arises at far ranges when the radar beam is wider than the mesocyclone's core diameter; characteristics of the mesocyclone are degraded to such an extent that neither the size nor strength of the mesocyclone is recoverable.

The tornadic vortex signature is the subject of this paper. One can study the theoretical characteristics of a TVS by scanning a simulated Doppler radar past a simulated tornado. To a first approximation, the tangential velocity distribution across a tornado can be simulated using an axisymmetric Rankine combined vortex (e.g., Brown and Wood 1991). A Rankine combined vortex

---

*Corresponding author address:* Dr. Rodger A. Brown, National Severe Storms Laboratory, 1313 Halley Circle, Norman, OK 73069.  
E-mail: brown@nssl.noaa.gov

consists of tangential velocity that increases linearly from zero at the center of the vortex to a maximum value at the core radius and then decreases, with velocity being inversely proportional to distance from the center.

The relationship between a simulated tornado's tangential velocity profile (Rankine combined vortex) and a simulated Doppler velocity azimuthal profile (TVS) through the center of the tornado is illustrated in Fig. 1. The pointed curve that peaks at  $100 \text{ m s}^{-1}$  is the Rankine combined velocity profile for a tornado with a core radius of  $0.25 \text{ km}$  (from center to pointed peak). The curve with the rounded peaks represents the Doppler velocity TVS if the radar were able to make measurements in a continuous manner across the vortex; in this example, the radar's beamwidth is five times larger than the tornado's core radius. The data points represent the ordinary situation where Doppler velocity measurements are made at uniform azimuthal intervals. In this discussion, it is assumed that the azimuthal interval between data points is roughly equal to the radar beamwidth, as is the case with the National Weather Service's WSR-88D radars and with many research radars.

Figure 1 shows two possible placements of Doppler velocity measurements along the continuous TVS curve that have peak values of  $\pm 38 \text{ m s}^{-1}$  (Doppler velocity difference,  $\Delta V$ , of  $76 \text{ m s}^{-1}$ ). When one of the radar sample volumes coincides with the center of the tornado (such as datapoint C in Fig. 1a), the extreme Doppler velocity values that form the prominent part of the TVS (points B and D) are separated by two azimuthal intervals. The difference between the extreme Doppler velocity values is  $58 \text{ m s}^{-1}$ , so the apparent peak velocities of the TVS are  $58/2 = \pm 29 \text{ m s}^{-1}$ . If one were computing the conventional "gate-to-gate" velocity difference at adjacent azimuths (B-C or C-D), the  $\Delta V$  value would be only  $29 \text{ m s}^{-1}$ , with the apparent peak velocity being  $\pm 14.5 \text{ m s}^{-1}$ . These numbers are tabulated in Table 1.

At the other extreme, when the center of the tornado is midway between two sample volumes, the extreme Doppler velocity measurements are separated by one azimuthal interval (datapoints H and I in Fig. 1b). In this case,  $\Delta V = 74 \text{ m s}^{-1}$  and the apparent peak velocity of the TVS is  $74/2 = \pm 37 \text{ m s}^{-1}$ . The gate-to-gate approach produces the same values for  $\Delta V$  and  $\bar{V}$  (see Table 1), because the extreme data points are adjacent to each other. Random placement of the uniformly spaced data points between the two extremes shown in Fig. 1, as occurs in actual radar measurements, results in apparent peak velocities between  $\pm 29$  and  $\pm 37 \text{ m s}^{-1}$ , and gate-to-gate peak velocities between  $\pm 14.5$  and  $\pm 37 \text{ m s}^{-1}$  (compared with the actual TVS peak velocity of  $\pm 38 \text{ m s}^{-1}$ ).

The two random sample positions of the data points in Figs. 1a and 1b relative to the peaks of the continuous TVS curve indicate that the process of radar sampling affects the estimation of the apparent peak velocity associated with a TVS, as discussed more fully by Wood

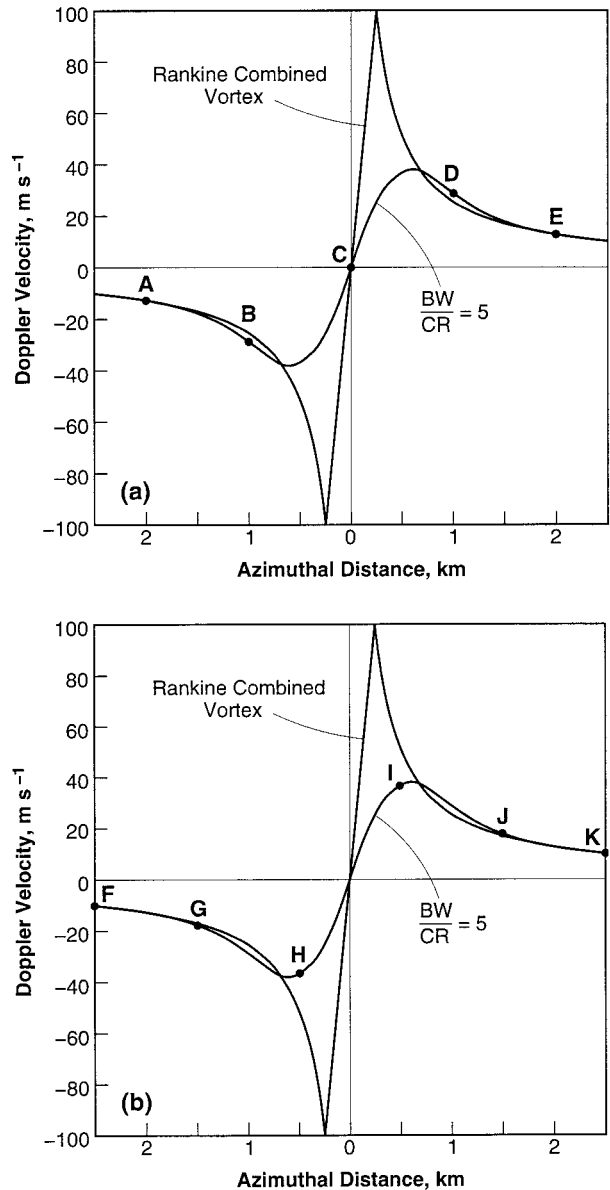


FIG. 1. Continuous (rounded-peaked curve) and discrete (data points labeled A-E, F-K) representations of a tornadic vortex signature (TVS) based on simulated Doppler velocity azimuthal profiles across the center of a simulated tornado (i.e., Rankine combined vortex; pointed-peaked curve that peaks at  $100 \text{ m s}^{-1}$ ). The continuous TVS curve represents the situation when the width of the radar beam is five times larger than the tornado's core radius. Shown are two of the many potential placements of radar sample volumes (spaced at uniform azimuthal intervals) when a radar scans across the center of a tornado: (a) one sample volume (C) coincides with the center of the tornado and (b) the tornado center is midway between two sample volumes (H and I). After Brown and Lemon (1976) and Wood and Brown (1997).

and Brown (1997). In this example, we see (a) a difference of  $8 \text{ m s}^{-1}$  between the extreme estimates of the peak TVS velocity (a difference of  $16 \text{ m s}^{-1}$  for  $\Delta V$ ), (b) a difference of over  $22 \text{ m s}^{-1}$  between the more

TABLE 1. Comparisons of peak TVS velocity difference ( $\Delta V$ ) and average peak TVS value ( $\bar{V}$ ) for the continuous TVS curve in Fig. 1 with values estimated from the data points in Figs. 1a and 1b. The apparent peak values are based on the extreme data point values (separated by one or two azimuthal intervals), while the “gate-to-gate” values are based on adjacent extreme data point values (separated by one azimuthal interval).

Data	Actual peak values (peak to peak) $\Delta V/\bar{V}$	Apparent peak values (extreme data points) $\Delta V/\bar{V}$	“Gate-to-gate” values (adjacent extremes) $\Delta V/\bar{V}$
Fig. 1a	76/±38 m s <sup>-1</sup>	58/±29 m s <sup>-1</sup>	29/±14.5 m s <sup>-1</sup>
Fig. 1b	76/±38 m s <sup>-1</sup>	74/±37 m s <sup>-1</sup>	74/±37 m s <sup>-1</sup>

restrictive gate-to-gate estimate of the peak TVS velocity (a difference of 45 m s<sup>-1</sup> for  $\Delta V$ ) and (c) that all of the estimates underestimate the actual peak velocity. Thus, gross underestimations will occur with gate-to-gate estimates when the center of the radar beam is nearly coincident with the center of a tornado.

The purpose of this paper is to present a procedure whereby an investigator can reasonably estimate the peak of the TVS curve (±38 m s<sup>-1</sup> in the above example) based on a set of data points randomly positioned along the curve (as those in Figs. 1a or 1b). Being able to do this is important when one is trying to determine how a TVS is evolving as part of a study undertaken by operational or research meteorologists. This procedure also permits the investigator to estimate the azimuth of the center of the corresponding tornado within 0.1°–0.2°.

## 2. TVS simulations

### a. Assumptions

As mentioned in the introduction, the tornado model upon which the simulated TVS curves are based is the Rankine combined velocity profile (Fig. 1). Close-range measurements of tornadoes by the Doppler on Wheels (DOW) during the 1995 Verification of the Origins of Rotation in Tornadoes Experiment in the southern plains revealed details of tornadic and parent circulations because the radar beamwidth was much smaller than the size of the circulations (e.g., Straka et al. 1996; Wurman et al. 1996). At first glance, these data suggest that the Rankine profile is an acceptable one for the observed tornadoes; however, more research needs to be done to accurately determine the observed profiles.

Because the Rankine profile represents a simple axisymmetric vortex, it does not account for such characteristics as radial inflow in the lowest few tens of meters above the ground, smaller-scale subvortices around the edge of the overall tornado circulation, the presence of a larger parent circulation, etc. Since this paper discusses the TVS, which occurs when the radar beam is larger than the tornado and therefore when the radar is some distance from the tornado, then (a) the radar beam at its lowest elevation angle is too high above the ground to detect the shallow radial inflow and (b) the small-scale subvortices are completely smeared

by the much larger radar beam into the overall tornadic vortex signature.

Parent circulations larger than the radar’s beamwidth will cause departures from a Rankine profile at the outer edges of a tornado. At times, the detailed DOW measurements taken within 10–12 km of tornadoes revealed the existence of a vortex that was slightly larger and weaker than the tornado and smaller than the parent mesocyclone (e.g., Straka et al. 1996); it is too early to know how often this intermediate vortex is present. In the radar measurements discussed in this paper, the broad radar beam smears the tornado to produce the prominent portion of the TVS. The contribution of the background mesocyclone at the outer edges of a TVS is taken into consideration in the discussion that follows.

### b. TVS curves

Realistic TVS data can be simulated by scanning a simulated radar through the Rankine combined vortex model of a tornado (e.g., Zrnić and Doviak 1975; Wood and Brown 1997). Generic radar characteristics of the typical 10-cm-wavelength research or WSR-88D radar can be used for the simulations. Variations among individual radars are normalized by dividing the azimuthal separation of Doppler velocity data points by the beamwidth of the individual radar. In this way, the simulated radar results can be applied to any horizontally scanning pulse Doppler radar.

Various TVS curves produced by the simulated radar collecting data continuously in azimuth are shown in Fig. 2. The curves represent Doppler velocity measurements in a tornado having a peak tangential velocity of 100 m s<sup>-1</sup> for various ratios of radar beamwidth (BW) to core radius (CR) of the simulated tornado; core radius is defined as the radius of the tornado’s maximum tangential velocity. When the BW/CR ratio is 3, for example, the peak TVS value is only 53% of the tornado’s peak tangential velocity. With the curves in Fig. 2 plotted as a function of azimuthal distance divided by beamwidth, a basic feature of the TVS is evident; namely, as a tornado’s core diameter decreases relative to the beamwidth, the peak-to-peak diameter of the TVS does not become any smaller than approximately one beamwidth, regardless of tornado size or strength.

As mentioned, the curves presented in Fig. 2 represent data collected continuously in azimuth. However, Dopp-

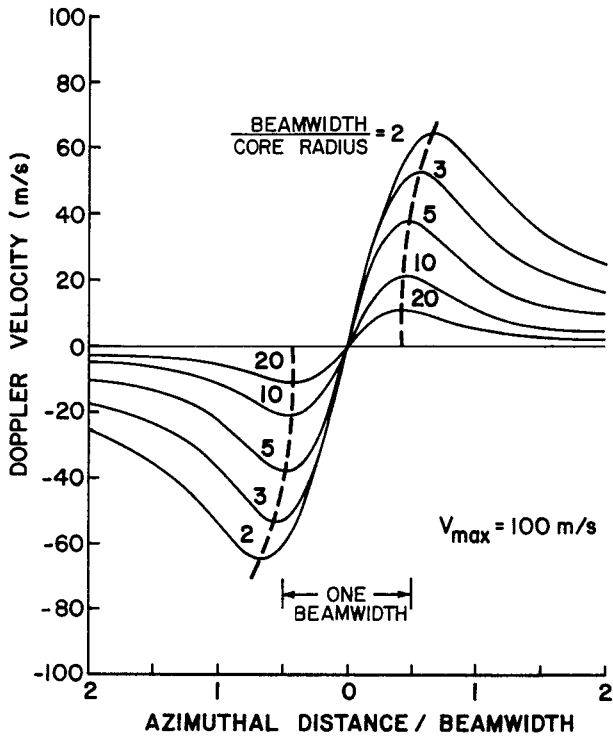


FIG. 2. Theoretical Doppler velocity profiles for a radar scanning in a continuous manner through the center of a tornado for various beamwidth to core radius (BW/CR) ratios. The TVS curves are plotted as a function of azimuthal distance divided by the radar's effective beamwidth. Maximum tangential velocity ( $V_{max}$ ) in the simulated tornado is  $100 \text{ m s}^{-1}$ . From Brown et al. (1978).

ler radar measurements are not continuous in azimuth. For example, the operational Weather Surveillance Radar-1988 Doppler (WSR-88D) collects data at azimuthal intervals of basically  $1.0^\circ$ . Owing to the WSR-88D's fast rotation rate, the nominal  $0.93^\circ$  beamwidth is broadened to a nominal effective beamwidth of about  $1.29^\circ$  (this value is derived in the appendix). Owing to the random placement of radar sampling volumes relative to the peaks of the TVS curve, it would be unusual for data points to be near both peaks (as in Fig. 1b). It is more likely that either one peak or neither peak will be well sampled.

**3. A nomogram for estimating the peak velocity of a TVS**

Brown et al. (1978) showed that Doppler velocity measurements in the 1973 Union City, Oklahoma, tornado and 1975 Stillwater, Oklahoma, tornado fitted theoretical TVS curves derived from Fig. 2. Figure 3 shows the locations of the Doppler velocity data in the Union City TVS after the data points were adjusted in azimuth and velocity relative to the vortex center; the research radar was moving so slowly that the beamwidth was not noticeably broadened during data collection. The

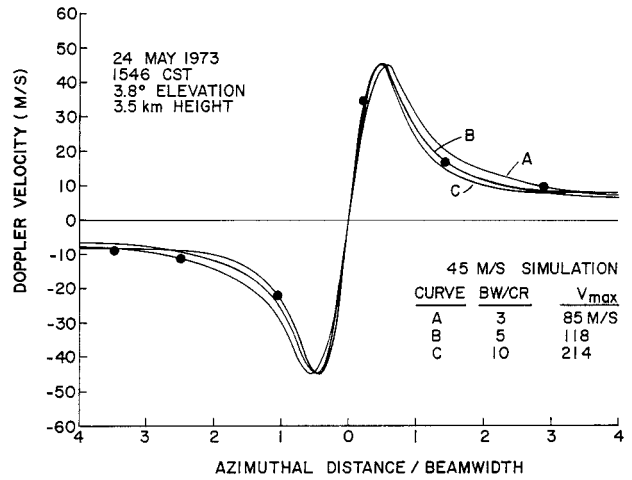


FIG. 3. Theoretical Doppler velocity profiles through the center of the Union City, OK, tornadic vortex signature. The three curves (derived from Fig. 2) represent vortices with various maximum tangential velocities ( $V_{max}$ ) chosen to produce extreme TVS values of  $\pm 45 \text{ m s}^{-1}$ . Dots are observed Doppler velocity values. From Brown et al. (1978).

three curves shown in the figure are the BW/CR = 3, 5, and 10 curves from Fig. 2 where the TVS peak velocity is  $45 \text{ m s}^{-1}$ . For example, the BW/CR = 5 curve in Fig. 2 would have a peak value of  $45 \text{ m s}^{-1}$  if the existing TVS peak of  $38 \text{ m s}^{-1}$  were multiplied by 1.18. This means that the tornado in which the Doppler radar is making the measurements has a peak tangential velocity of  $1.18 \times 100 \text{ m s}^{-1} = 118 \text{ m s}^{-1}$ . Without a reliable independent estimate of the core radius at the radar sampling altitude, we are not able to use this approach to deduce the peak tangential velocity in the tornado. The three nearly identical curves in Fig. 3 represent three distinctly different tornadoes: (a)  $V_{max} = 85 \text{ m s}^{-1}$  when the beamwidth is 3 times the tornado's core radius, or (b)  $V_{max} = 118 \text{ m s}^{-1}$  when the beamwidth is 5 times the core radius, or (c)  $V_{max} = 214 \text{ m s}^{-1}$  when the beamwidth is 10 times the core radius.

The curves in Fig. 2 were used, following the example in Fig. 3, to construct a nomogram consisting of a family of curves to represent various peak Doppler velocities for TVSs (Fig. 4). Each curve in Fig. 4 is an average of three curves having the same peak TVS velocity for BW/CR values of 3, 5, and 10. The procedure is to fit the measured TVS data points to these curves and thereby estimate the peak Doppler velocity value along the TVS curve. The first step is to plot the Doppler velocity values of a suspected TVS on a grid, like the one shown in Fig. 5. The vertical lines have a normalized azimuthal separation of 0.775 (azimuthal interval of  $1.0^\circ$  divided by the nominal effective beamwidth of  $1.29^\circ$ ), so they represent normalized intervals that are consistent with the curves in Fig. 4. One of the data points near the center of the TVS (e.g., B, C, or D in Fig. 1a, or H or I in Fig. 1b) is plotted on the vertical line labeled 0.

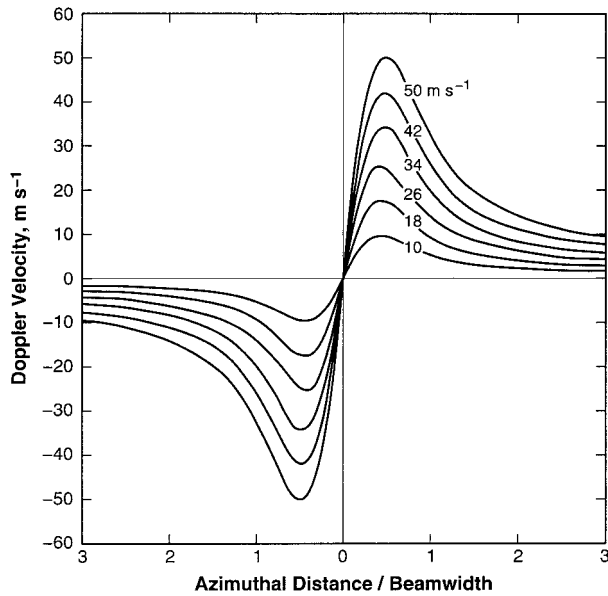


FIG. 4. Nomogram showing azimuthal variation (normalized by effective beamwidth) of theoretical TVS curves labeled according to the peak value of each curve.

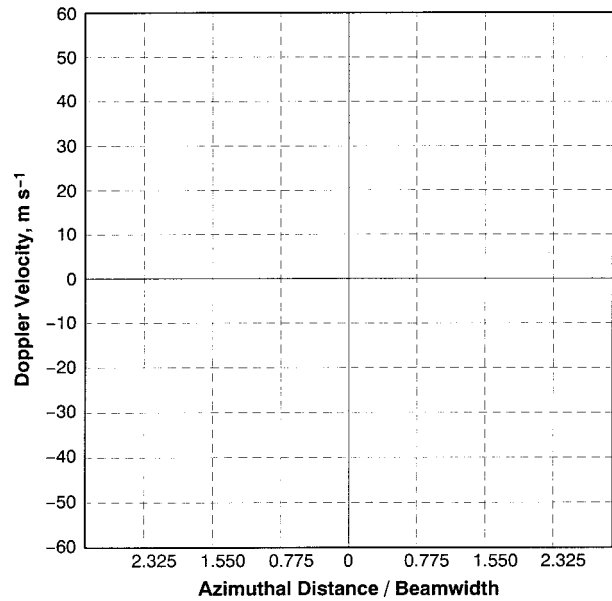


FIG. 5. Nominal grid for plotting WSR-88D Doppler velocity data points in a TVS. Vertical lines represent the normalized spacing between adjacent data points for a WSR-88D radar having mean characteristics (see discussion in the text).

Then Doppler velocity data to the right (clockwise azimuthal direction) and left (counterclockwise) of that point are plotted on the adjacent vertical lines.

#### 4. TVS peak velocities associated with the Garden City, Kansas, tornado of 16 May 1995

On 16 May 1995, an evolving supercell thunderstorm produced a series of tornadoes for three hours as it moved from Garden City east-northeastward to Rozel in southwestern Kansas. The subject of this study is the first tornado, which passed just southeast of Garden City. According to *Storm Data* (NCDC 1995), the tornado was on the ground for 19 min.

Figure 6 shows a plot of TVS data points collected by the Dodge City (KDDC) WSR-88D radar as the radar scanned through the Garden City tornado at about 2323 UTC. The size of the data points reflects the typical amount of uncertainty in the mean Doppler velocity values owing to the broad spectrum of within-beam velocities in the vicinity of a tornado. Using Fig. 6.5 of Doviak and Zrnić (1993), and assuming that the spectrum width associated with the typical TVS is 10–16  $m s^{-1}$  and that the Nyquist velocity is between 25 and 32  $m s^{-1}$ , the nominal accuracy of 0.7  $m s^{-1}$  increases to 1.4 to 5.3  $m s^{-1}$ , with an average value of 2.5  $m s^{-1}$ . The plotted data points, therefore, are 5  $m s^{-1}$  in the vertical and, by making them circular, a small uncertainty in the azimuthal value is also acknowledged.

The peak Doppler velocity value of the appropriate TVS curve can be estimated by adjusting the theoretical nomogram curves (Fig. 4) as a transparent overlay on

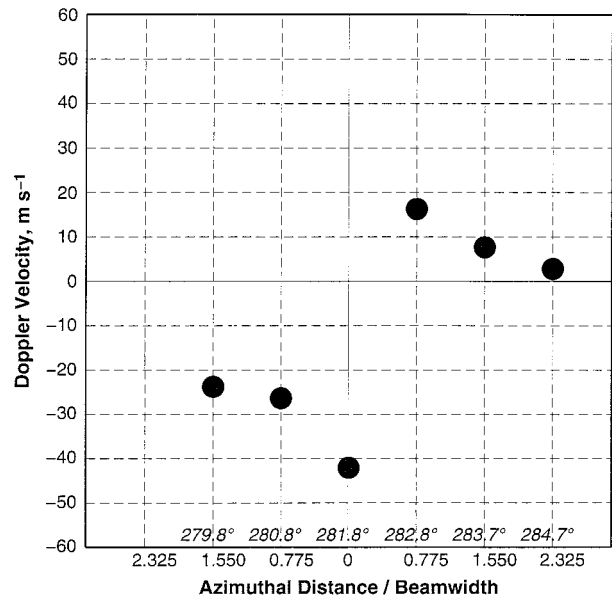


FIG. 6. Plot of six data points measured within a TVS by the KDDC WSR-88D radar as it scanned through the Garden City, KS, tornado at about 2323 UTC on 16 May 1995 at 77.9 km range and 2.4° elevation angle (3.6 km height). Data point size indicates measurement accuracy. The azimuth angle (°) of each data point is listed along the bottom of the grid. The full-resolution data were obtained by replaying an archive level II data tape.

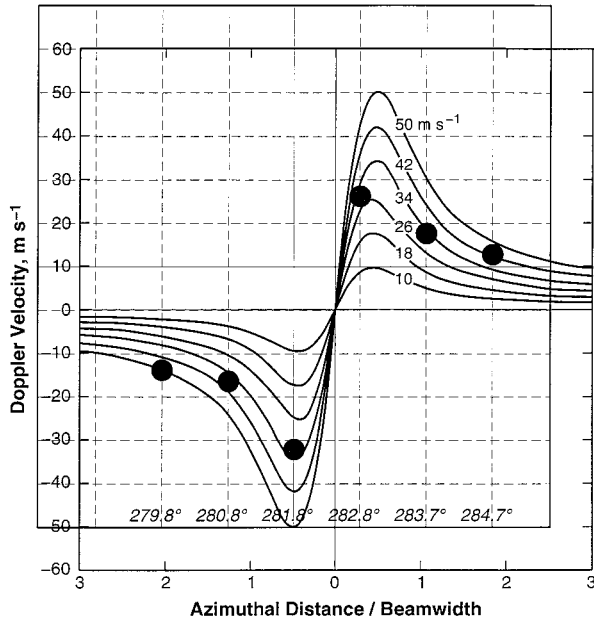


FIG. 7. Superposition of Figs. 4 and 6 to produce the best fit for the three data points closest to the vortex center.

top of the plotted data points in Fig. 6. The adjustment process consists of the following steps:

- 1) the nomogram curves are moved up or down to subtract the contribution due to tornado and storm motion;
- 2) the nomogram curves are moved to the left or right to permit proper fit of the data points relative to the tornado center; and
- 3) the final adjustment is the best fit of the curves to the data points.

Typically, only the three or four data points closest to the TVS center fit one of the curves or lie the same proportional distance between two curves. A minimum of three data points is required. Data points farther from the center may depart from the TVS curve owing to a contribution from the background mesocyclone. If the TVS is strong and overpowers the parent mesocyclone signature (as in Fig. 3), all the TVS points should be in the same position relative to the curves.

The final position of the theoretical TVS curves on top of the KDDC data points is shown in Fig. 7. Because at least the three centermost data points fit the curves and the outermost points decrease in magnitude with distance from the vortex center, we can be confident that this feature is a TVS. The peak of the TVS curve is approximately  $\pm 33 \text{ m s}^{-1}$ , as compared with a measured peak value of only  $\pm 29 \text{ m s}^{-1}$ , based on the average of the measured extreme values of +16 and  $-42 \text{ m s}^{-1}$ . The shift of the curves downward by  $10 \text{ m s}^{-1}$  indicates that an overall Doppler component of  $10 \text{ m s}^{-1}$  toward

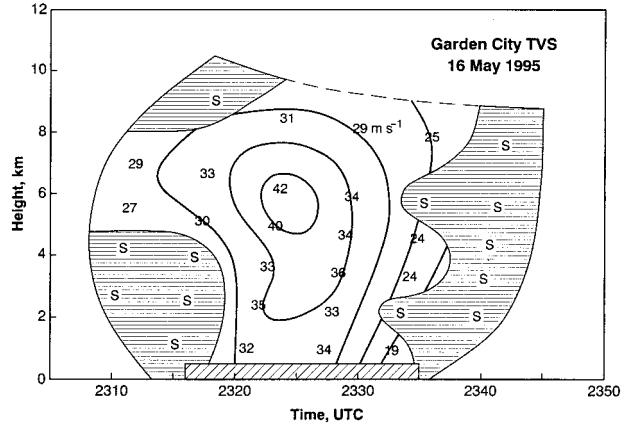


FIG. 8. Time–height plot of the estimated peak values of TVS curves associated with the Garden City tornado. The shaded areas represent marked shear (S) regions where Doppler velocity values did not fall off with azimuth like the theoretical TVS curves do, suggesting the presence of a marked cyclonic shear zone rather than a vortex. The contour interval is  $5 \text{ m s}^{-1}$ . The hatched bar along the bottom indicates when the tornado was on the ground according to *Storm Data* (NCDC 1995).

the radar (owing primarily to tornado and storm motion) was superimposed on the basic TVS Doppler velocities.

In some cases, there can be two equally probable fits of three adjacent data points to the theoretical curves. When this occurs, the estimated tornado center remains between the same two extreme Doppler velocity values, but is shifted by a few tenths of a degree. One solution has the closest data point on the left side of the tornado center and the other has the closest point on the right side of the center. In this situation, an average is taken of the two estimated peak values.

In addition to estimating the peak Doppler velocity value associated with a TVS, the center azimuth (to the nearest  $0.1^\circ$ – $0.2^\circ$ ) for the TVS, and therefore for the tornado, can be determined from Fig. 7. The center of the Garden City tornado was at a range of 77.9 km and azimuth of about  $282.4^\circ$  at the height and time of these measurements.

Figure 8 shows a time–height plot of the estimated peak values of the TVS curves during the lifetime of the Garden City tornado, based on the nomogram approach. The uncertainty of a meter per second or two in the peak velocity estimates was taken into account in the drawing of the contour lines. Within the shaded regions, TVS-like cyclonic shear (S) was present, but the Doppler velocity values on one or both sides of the velocity discontinuity remained essentially constant. These characteristics indicate the presence of a marked cyclonic shear zone rather than a vortex.

Evolution of the TVS is consistent with the reported duration of the tornado on the ground (hatched bar at the bottom of Fig. 8); although tornado times reported in *Storm Data* can be in error, they appear to be very reasonable in this case. The data indicate that the TVS

TABLE A1. Range and overall mean of WSR-88D effective horizontal beamwidth values  $\theta_e$  as a function of VCP, Nyquist velocity  $V_N$ , antenna rotation rate  $\alpha$ , number of sampled pulses  $M$ , and pulse repetition period  $T$ . From Wood and Brown (1997).

VCP	$V_N$ ( $\text{m s}^{-1}$ )	$\alpha$ ( $^\circ \text{ s}^{-1}$ )	$M$ (pulses)	$T$ (ms)	$\theta_e$ ( $^\circ$ )
11	25	16.1–19.2	41–52	1.06	1.174–1.461
11	32	16.1–19.2	50–66	0.83	1.151–1.453
21	25	11.2–11.4	70–88	1.06	1.268–1.461
21	32	11.2–11.4	88–111	0.83	1.257–1.448
				Mean	1.29

formed at midaltitudes in a region of strong cyclonic shear and remained strongest/largest aloft during its entire lifetime. Evolution of TVS peak values reasonably indicates that the tornado became stronger and/or larger during the first half of its existence and then became weaker and/or smaller during the latter half; this evolution is similar to those of gate-to-gate TVSs documented by Vasiloff (1993).

It is customary to prepare time–height plots of either the difference between the measured gate-to-gate TVS values or the average of the gate-to-gate values (one-half the difference). When either of these approaches is used, the values at one particular time can be less than those at adjacent times (e.g., Vasiloff 1993), giving the impression that the tornado momentarily weakened. In these situations, it is likely that one of the azimuthal data points was centered on the tornado and, using gate-to-gate values, only half of the full velocity difference (across two azimuthal intervals) was used; the middle and right columns for Fig. 1a data in Table 1 illustrate this type of problem. The nomogram approach discussed in this paper compensates for this and other sampling problems.

Differences were computed between (a) the peak TVS value deduced using the nomogram approach (e.g.,  $\pm 33 \text{ m s}^{-1}$  based on Fig. 7) and (b) the average of the measured extreme TVS values (e.g.,  $\pm 29 \text{ m s}^{-1}$  based on Fig. 6) for all the data points in Fig. 8; in this particular dataset, all of the extreme Doppler velocity values were separated by one azimuthal interval. The estimated peak values of the TVS curves always were larger than the averages of the extreme measured values, with differences ranging from 2 to 9  $\text{m s}^{-1}$ .

## 5. Concluding comments

A technique has been discussed that deduces the peak value of the TVS curve based on Doppler velocity measurements that, by their nature, are randomly positioned relative to the peaks of the curve. The approach is to compare the Doppler velocity values within a suspected TVS with a set of theoretical TVS curves. If at least the three data points closest to the vortex center fit the curves, and the other points decrease with distance from the center, then the peak value associated with the TVS can be estimated. Use of this approach in TVS studies (using reproduced copies of Fig. 4 and reproduced or

recomputed copies of Fig. 5) can produce peak TVS velocities that are more consistent in time and height than those computed directly from the extreme measured values, especially when gate-to-gate values are used. The feasibility is being explored of incorporating an automated version of this technique into the WSR-88D algorithm that is used to detect tornadic vortex signatures.

*Acknowledgments.* Timothy Burke of the Cooperative Institute for Mesoscale Meteorological Studies assisted with the processing of the Garden City TVS data. The helpful comments of Dr. Jeffrey Trapp and of the anonymous reviewers are most appreciated. Joan O'Bannon ably produced the figures that were not borrowed from other publications. Christine Sweet provided valuable editorial assistance.

## APPENDIX

### Effective Beamwidths for WSR-88D Radars

When a radar antenna moves azimuthally a significant angular distance while transmitting the number of pulses required to compute a representative Doppler velocity value, the antenna beamwidth is effectively broadened in the azimuthal direction (e.g., Doviak and Zrnić 1993). With rotation rates of 11–19  $\text{s}^{-1}$  for volume coverage patterns (VCP) 11 and 21 that are used in severe thunderstorm data collection modes, WSR-88D radars experience considerable beamwidth broadening during the acquisition of tornadic vortex signatures (e.g., Wood and Brown 1997). Among the various WSR-88D radars, the transmitted wavelength varies from 10.0 to 11.1 cm (mean 10.6 cm) and the half-power beamwidth varies from 0.88 $^\circ$  to 0.97 $^\circ$  (mean 0.93 $^\circ$ ), (S. Smith 1996, personal communication), WSR-88D Operational Support Facility, Norman, Oklahoma. For a given radar, the antenna rotation rate  $\alpha$ , number of pulses  $M$  used to compute the mean Doppler velocity value, pulse repetition period  $T$ , and Nyquist velocity  $V_N$  can vary from elevation angle to elevation angle for a given VCP.

Table A1 shows the range of effective beamwidth  $\theta_e$  values for the two VCP modes and typical extreme Nyquist velocities  $V_N$  of 25 and 32  $\text{m s}^{-1}$ . For these computations, the mean wavelength and mean beamwidth were used;  $T$  was computed from the mean wavelength

and  $V_N$ . The range of values for  $\alpha$  and  $M$  are those specified for elevation angles less than  $7^\circ$  (NWS 1992), which encompass TVS depth at most ranges of interest. Though the values of  $\alpha$ ,  $M$ , and  $T$  varied by up to a factor of 2 or more, the variations were in opposite senses such that all of the effective beamwidth values were within 13% of the overall mean effective beamwidth of  $1.29^\circ$ .

Instead of using the nominal plotting chart in Fig. 5, one can prepare a plotting chart that is tailored to any radar and its specific operating mode by recomputing the placement of the vertical lines in Fig. 5. The effective beamwidth can be computed from an equation, or read from a figure, given in section 7.8 of Doviak and Zrnić (1993) using specific values of  $\alpha$ ,  $M$ ,  $T$ , and antenna beamwidth.

#### REFERENCES

- Brown, R. A., and L. R. Lemon, 1976: Single Doppler radar vortex recognition: Part II—Tornadic vortex signatures. Preprints, *17th Conf. on Radar Meteorology*, Seattle, WA, Amer. Meteor. Soc., 104–109.
- , and V. T. Wood, 1991: On the interpretation of single-Doppler velocity patterns within severe thunderstorms. *Wea. Forecasting*, **6**, 32–48.
- , L. R. Lemon, and D. W. Burgess, 1978: Tornado detection by pulsed Doppler radar. *Mon. Wea. Rev.*, **106**, 29–38.
- Donaldson, R. J., Jr., 1970: Vortex signature recognition by a Doppler radar. *J. Appl. Meteor.*, **9**, 661–670.
- Doviak, R. J., and D. S. Zrnić, 1993: *Doppler Radar and Weather Observations*. Academic Press, 562 pp.
- NCDC, 1995: *Storm Data*. Vol. 37, No. 5, 268 pp. [Available from National Climatic Data Center, Asheville, NC 28801.]
- NWS, 1992: Operation instructions Unit Control Position (UCP), Doppler meteorological radar WSR-88D. NWS Manual EHB 6-521, 577 pp. [Available from NOAA Logistics Supply Center, Kansas City, MO 64131.]
- Straka, J. M., J. Wurman, and E. N. Rasmussen, 1996: Observations of the low-levels of tornadic storms using a portable X-band Doppler radar. Preprints, *18th Conf. on Severe Local Storms*, San Francisco, CA, Amer. Meteor. Soc., 11–16.
- Vasiloff, S. V., 1993: Single Doppler radar study of a variety of tornado types. *The Tornado: Its Structure, Dynamics, Prediction, and Hazards, Geophys. Monogr.*, No. 79, Amer. Geophys. Union, 223–232.
- Wood, V. T., and R. A. Brown, 1997: Effects of radar sampling on single-Doppler velocity signatures of mesocyclones and tornadoes. *Wea. Forecasting*, **12**, 929–939.
- Wurman, J., J. Straka, and E. Rasmussen, 1996: Preliminary radar observations of the structure of tornadoes. Preprints, *18th Conf. on Severe Local Storms*, San Francisco, CA, Amer. Meteor. Soc., 17–22.
- Zrnić, D. S., and R. J. Doviak, 1975: Velocity spectra of vortices scanned with a pulse-Doppler radar. *J. Appl. Meteor.*, **14**, 1531–1539.